A Heterogeneous Sensing Suite for Multisymptom Quantification of Parkinson's Disease

Weiguang Huo, Paolo Angeles, Yen F. Tai, Nicola Pavese, Samuel Wilson, Michele T. Hu, and Ravi Vaidyanathan

***Abstract*— Parkinson's disease (PD) is the second most common neurodegenerative disease affecting millions worldwide. Bespoke subject-specific treatment (medication or deep brain stimulation (DBS)) is critical for management, yet depends on precise assessment cardinal PD symptoms - bradykinesia, rigidity and tremor. Clinician diagnosis is the basis of treatment, yet it allows only a cross-sectional assessment of symptoms which can vary on an hourly basis and is liable to inter- and intra-rater subjectivity across human examiners. Automated symptomatic assessment has attracted significant interest to optimise treatment regimens between clinician visits, however, no wearable has the capacity to simultaneously assess all three cardinal symptoms. Challenges in the measurement of rigidity, mapping muscle activity out-of-clinic and sensor fusion have inhibited translation. In this study, we address all through a novel wearable sensor system and machine learning algorithms. The sensor system is composed of a force-sensor, three inertial measurement units (IMUs) and four custom mechanomyography (MMG) sensors. The system was tested in its capacity to predict Unified Parkinson's Disease Rating Scale (UPDRS) scores based on quantitative assessment of bradykinesia, rigidity and tremor in PD patients. 23 PD patients were tested with the sensor system in parallel with exams conducted by treating clinicians and 10 healthy subjects were recruited as a comparison control group. Results prove the system accurately predicts UPDRS scores for all symptoms (85.4% match on average with physician assessment) and discriminates between healthy subjects and PD patients (96.6% on average). MMG features can also be used for remote monitoring of severity and fluctuations in PD symptoms out-of-clinic. This closed-loop feedback system enables individually tailored and regularly updated treatment, facilitating better outcomes for a very large patient population.**

***Index Terms*— Parkinson's disease symptoms, wearable sensor system, machine learning, MMG, telemedicine, muscle stiffness.**

Manuscript received October 9, 2019; revised January 24, 2020; accepted February 10, 2020. Date of publication April 13, 2020; date of current version June 5, 2020. This work was supported in part by the UK EPSRC under Grant EP/R511547/1, in part by the UK EPSRC Imperial College London Centre for Doctoral Training in Neruotechnology, in part by the UK Dementia Research Institute Care Research and Technology (DRI-CRT) Centre, in part by the UKIERI under Grant 2016-17-0103, and in part by Serg Technologies. *(Corresponding author: Weiguang Huo.)*

Weiguang Huo and Ravi Vaidyanathan are with the Department of Mechanical Engineering, Imperial College London, London SW7 2AZ, U.K., and also with the UK Dementia Research Institute-Care Research and Technology Centre, Imperial College London, London SW7 2AZ, U.K. (e-mail: w.huo@imperial.ac.uk; r.vaidyanathan@imperial.ac.uk).

Paolo Angeles and Samuel Wilson are with the Department of Mechanical Engineering, Imperial College London, London SW7 2AZ, U.K. (e-mail: paolo.angeles09@imperial.ac.uk; s.wilson14@imperial.ac.uk).

Yen F. Tai is with the Department of Neurology, Charing Cross Hospital, Imperial College London, London W6 8RF, U.K. (e-mail: yen.tai@imperial.ac.uk).

Nicola Pavese is with the Clinical Ageing Research Unit, Newcastle University, Newcastle upon Tyne NE4 5PL, U.K. (e-mail: nicola.pavese@ncl.ac.uk).

Michele T. Hu is with the Department of Neurology, Nuffield Department of Clinical Neurosciences, University of Oxford, Oxford OX3 9DU, U.K. (e-mail: michele.hu@ndcn.ox.ac.uk).

Digital Object Identifier 10.1109/TNSRE.2020.2978197

I. Introduction

PARKINSON'S disease (PD) is the second most common neurodegenerative disorder [1], with 130,000+ UK patients and 10 million+ worldwide [2]. PD results primarily from the death of dopaminergic neurons in the substantia nigra [3]. The disease manifests itself in three cardinal symptoms, tremor, bradykinesia and rigidity [4] with several other associated patient effects (dementia, impaired posture, impaired speech, etc). Cardinal symptoms respond to treatment with dopamine replacement therapy at early stages of the disease. As it progresses, deep brain stimulation (DBS) of the subthalamic nucleus (STN) has been used as an effective treatment of PD patients with refractory fluctuations [5]–[9], though treatment of manifestations such as tremor can complicate other movement disorders such as dystonia [10], underscoring the need to treat multiple manifestations of Parkinsonism. Optimal placement of stimulation electrodes and precise parameterisation of stimulation parameters (e.g. frequency) can be challenging [8], [11], [12], and is normally dependent on diagnosis of subject-specific motor response through trial-and-error. Consequently, accurate monitoring and assessment of symptom severity are of great importance not only to treatment selection but also for adjustment of regimens (e.g. levodopa and STN-DBS) that must be tailored to each patient's symptomatic response.

Clinical assessment of PD symptom severity is usually based on rating scales, of which the Unified Parkinson's Disease Rating Scale (UPDRS) [13] is the most popular. However, the UPDRS scale is liable to inter- and intra-rater subjectivity

across PD examiners depending on their experience [14]. Moreover, treatment regimens are limited to a "snapshot" of symptom fluctuation during a clinical visit for patients with Parkinson's disease (PwPD), while the patient's response can vary tremendously throughout the day.

Wearable sensors have been widely studied with demonstrated positive impact in providing objectively accurate information of PwPD movements throughout a longitudinal view of symptom fluctuations out-of-clinic [7], [15]–[17]. Inertial sensors such as accelerometers and gyroscopes, for example, have been packaged as wearable devices to successfully measure bradykinesia [7], [18]–[20] and tremor (including kinetic, postural, and rest tremors) [21]–[24]. Features of angular velocity were proven to show a strong correlation to bradykinesia scores which is rated based on the decrementation level in the amplitude of repetitive movements, e.g., hand pronation/supination, finger tapping, and hand motions [7]. Accelerometers are the most frequently utilised sensor to measure tremor. Besides, angular velocities measured using gyroscopes attached on the forearms and/or fingers have also been proven as an effective means to quantify tremor [7], [25]. Their success reflects the capacity of the sensing modality to map all significant characteristics of tremor (amplitude, frequency) for severity assessment. Our previous work has expanded on this to create a system using accelerometers in a cell phone as an immediately available sensing tool [26]. In addition, a smaller body of work (e.g. [27]–[29]) has explored motion tracking for PwPD with vision. Camera data capture systems have the advantage of noncontact and parallel clinician visual assessment. However, they also require a controlled environment and suffer from occlusion (blocking) of the camera source. Beyond bradykinesia and tremor, rigidity remains a critical diagnostic feature in PD. Indeed, the capacity to modulate muscle stiffness is widely acknowledged as a vital measure of the integrity of the motor system [30]. Its degradation is a major manifestation of PD, however, motion sensing (inertial, vision) lacks the capacity to assess changes in rigidity. As such, investigations have prioritised viscoelastic properties (VEPs) and impedance of the limbs for PD assessment. Force and/or stiffness data has quantified rigidity on the elbow and wrist, which can be correlated to UPDRS scores [4], [31], [32]. Electromyography (EMG) measurements capturing physiological metrics of muscle activity have also shown promise at quantifying rigidity in PwPD [33]. It should be noted that diagnosis and treatment for PD, however, is usually based on observation of all cardinal symptoms. As such, investigators have argued [32] for the utility of an all-in-one sensor system, i.e., a system that measures all three of the cardinal motor symptoms. However, no such system has been demonstrated on PwPD. Commercially available sensor systems for PD diagnosis only measure one or two of the cardinal symptoms [34].

Quantification methods of PD symptoms can broadly be classified into two approaches. The first involves correlation of external sensor data to PD symptoms by creating a model based on the physical and physiological mechanisms of PD symptoms. This is then used as a basis for correlation

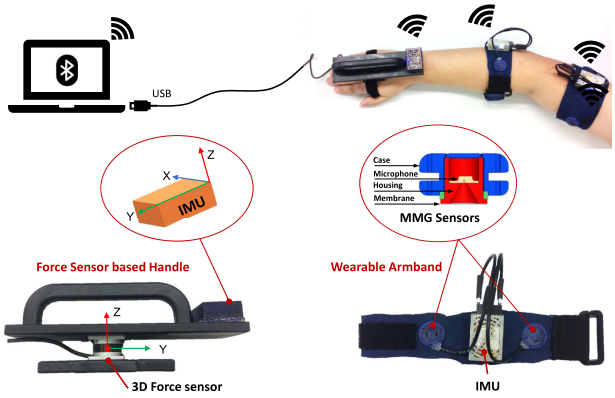

Fig. 1. Parkinson's diagnostic device (PDD).

to the UPDRS scores [35], [36]. The second approach is to extract sensor features and implement a regression/classification model to minimise the prediction errors to the UPDRS scores [37]–[40]. Since there exists no single model that has been explicitly defined to correlate UPDRS scores across all motor symptoms, machine learning algorithms are typically used as tools of analysis [41], [42].

In this paper, we present a new wearable Parkinson's diagnostic device (PDD) (Fig.1). New features of the system include the capacity: 1) to quantify all three primary PD motor symptoms (rigidity, tremor, and bradykinesia), 2) to fit smoothly into existing examination procedures for trivial introduction into practice, and 3) to be straightforward to use with no training in any environ (in or out-of-clinic). The first issue, capture of all symptoms, is addressed through the development of hardware for a multi-modal sensing suite capturing stiffness, muscle activity, and motion in a simple package that is trivial to wear and use. The sensor suite consists of four mechanomyography (MMG) sensors, three inertial measurement units (IMUs) and a force-sensor based handle. Although MMG is less mature than well-established EMG systems, it offers potential benefits versus EMG such as ease of application, higher signal-to-noise ratio, multiple (infinite) uses for a single sensor, immunity to changes in skin impedance, and elimination of the need of shaving and conductive gel all of which address simplicity and ease of use [43]. An inertial sensor fusion algorithm was implemented to combine movement and MMG data in one hardware package akin to wearables used for human-robot interface [44]. The PDD is easy to don and doff and requires no on-site calibration. Based on the measured signals using the PDD, features for each PD symptom were further extracted, and a machine-learning algorithm was developed to classify and predict the severity of three motor symptoms in PwPD according to the UPDRS scores rated by clinicians. The wearable PDD system was evaluated with 23 Parkinson's patients and 10 healthy subjects (control group). The results prove that the PDD can accurately estimate the PwPD's UPDRS scores for all PD motor symptoms with an average accuracy of 85.4% in a single exam akin to current clinical practice. The PDD further distinguishes the PwPD from healthy subjects with

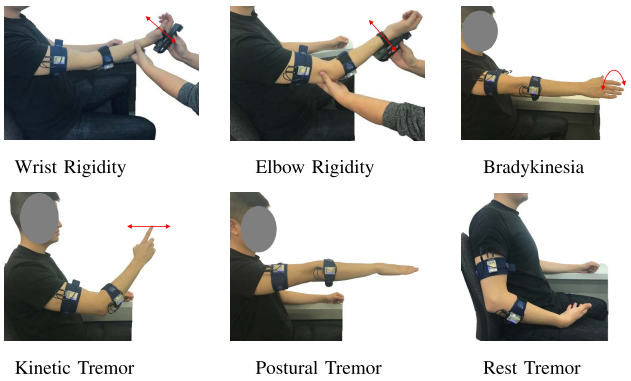

Fig. 2. A demonstration of the assessment procedure for each PD motor symptom.

an average accuracy of 96.6% across all symptoms. Clinical testing results demonstrate that incorporation of MMG signals can effectively improve symptom classification accuracy. Furthermore, comparison studies have shown promising results for detecting the UPDRS scores using only the IMU and MMG sensors, demonstrating MMG capacity to independently monitor rigidity which enables simple use in the home. To the best of our knowledge, this is the first wearable system to holistically measure the three cardinal symptoms of PD in one exam and the first successful implementation of MMG for PD system quantification.

II. Methods

A. Measurement System

In this study, we developed a novel PDD which consists of two wearable armbands and a force-sensor based handle (see Fig.1). The two armbands were worn at the patient's upper arm and forearm respectively, and the total weight of each armband is 100 g. The handle can be attached to the patient's hand or wrist using a strap, according to the diagnostic process (see Section II-B and Fig. 2). The handle was produced using a 3D printer and weights 200 g.

Each of the wearable armbands is composed of two MMG sensors and an IMU (STMicroelectronics, Switzerland), which contains a 3D accelerometer, a 3D gyroscope, a 3D magnetometer, and a small battery. The full scales of the accelerometer, gyroscope and magnetometer are ± 2 g, ± 500 degree/s and ± 2 Gauss, respectively. The MMG sensor was designed in Biomechatronics Lab, Imperial College London and is made of a micro-electro-mechanical microphone (Knowles, UK) housed in a 3D printed casing (see Fig.1) [43]. The handle was equipped with a compact 3D force sensor (Optoforce, UK) and an IMU (see Fig.1). The measured forces are up to ± 20 N in X and Y axes, 200 N in Z compression and 100 N in Z tension, which are sufficient to satisfy requirements for the rigidity assessment of the wrist and elbow joints. Prior studies have used a force sensor to measure rigidity but they were only able to record in one direction (the direction normal to movement) [31], [32]. By having two other directions to record any resistive force from, it is possible to construct a more holistic model of rigidity during UPDRS assessments as described in Section II-B.

TABLE I
Patients' Information

ID	Age	Sex	Symptoms	Side	H&Y	S-D	Setting
1	73	F	R^a, B, –	R	3	22	RCC
2	59	M	R^a, B, –	R	3	24	RCC
3	61	M	R^a, B, T^a	L	2	16	DBS
4	57	M	R^a, B, T^p	L	2	6	DBS
5	37	F	R^e, B, –	R	2	10	DBS
6	42	F	– B, $T^{p,r}$	R	1	16	DBS
7	43	F	R^a, B, T^k	R	5	7	DBS
8	61	M	R^a, B, $T^{p,r}$	R	3	8	DBS
9	52	F	R^a, B, T^p	R	2	7	DBS
10	50	M	– B, T^p	L	2	13	DBS
11	41	M	R^a, B, T^p	R	2	10	DBS
12	68	M	R^a, B, –	L	3	15	DBS
13	62	M	– – T^a	R	2	6	DBS
14	66	F	– – T^a	L	3	12	DBS
15	54	M	– – T^a	R	2	5	DBS
16	67	F	– B, –	L	3	13	DBS
17	51	F	R^a, B, –	R	2	8	RCC
18	69	M	R^a, B, –	R	3	17	RCC
19	71	F	R^a, – T^a	R	3	15	RCC
20	63	M	R^a, – T^a	R	2	5	DBS
21	70	F	R^a, B, T^a	R	2	10	RCC
22	53	M	– B, T^a	R	2	6	RCC
23	56	F	R^a, B, T^r	L	2	5	RCC

Side: most-affected side (L: Left, R: Right); H&Y: Hoehn & Yahr stage; S-D: symptom duration (unit: years)
Symptoms (R: Rigidity, superscript e and a: elbow and all; B: Bradykinesia; T: Tremor, superscript k, p, r, and a: kinetic, postural, rest, and all)
RCC: routine clinical check-up
DBS: deep brain stimulation programming session
Participation (elbow rigidity: [1-12, 17-23], wrist rigidity: [3-12, 17-23], bradykinesia: [3-12, 16, 18, 19, 21, 23], kinetic tremor: [3-11, 13, 15, 19-23], and postural/rest tremors: [3-11, 13-15, 19-23])

Each MMG sensor was connected to one of eight 10-bit analogue-to-digital converters of the IMU which was further connected to a host PC via Bluetooth. The MMG and IMU sensors can continuously record for up to 4 hours. The force sensor was connected to the PC by a USB port. The data measured from all sensors were synchronized and saved using a developed interface (in C#) at 100 Hz.

During the PD assessment, four MMG sensors were placed on the biceps brachii, triceps brachii, flexor carpi ulnaris and extensor carpi radialis longus, respectively. The arm and hand kinematics, such as the linear accelerations as well as the elbow and wrist joint angular velocities, can be efficiently measured using the IMU sensors. The force-sensor based handle was designed to measure the resistive force during the rigidity assessment alone, and was detached for bradykinesia and tremor assessments. The PDD system required no on-site calibration and did not require any preparation of the surface of the patient's skin. Moreover, it can be taken to any location for testing thanks to its portability.

B. Subjects and Procedures

23 patients with Parkinson's disease (see Table I) and 10 healthy subjects (Age: 27.6 ± 3 years old; Sex: 8 males and 2 females) participated in this study. Among of the patient cohort, the patient number in each symptom assessment is as follows: elbow rigidity: 19, wrist rigidity: 17, bradykinesia: 15, kinetic tremor: 16, and postural/rest tremors: 17. All healthy

subjects participated in all symptom assessments as the control group. Patients' data collection occurred across two different hospital sites: Charing Cross Hospital, London, UK and John Radcliffe Hospital, Oxford, UK in the two following settings: 1) after a routine clinical check-up (RCC); 2) during a DBS programming session (i.e., with DBS). 15 of the PwPD have received DBS, and the assessment was performed during DBS programming session. The stage and progression of the disease was not a limiting factor for this study. All subjects were given a patient information sheet regarding the assessment and gave written informed consent to all experimental procedures. This study received ethical approval from the Health Research Authority of the National Health Service (NHS), UK.

For all patients, only the most severely affected arm was tested during this study. The rigidity occurs at the elbow and wrist joints of the arm and therefore this assessment was split into two separate tests (see Fig. 2). Likewise for tremor, there are three types that can occur in PD, kinetic, postural and rest tremors. Each of the assessments was repeated three times with a break in-between to ensure that the patient did not fatigue quickly. Note that the same three-time assessments were repeated for a PD patient during DBS programming session when significant DBS settings were changed (i.e., electrode contact changes and large changes in stimulation intensity). All PD patients' symptoms were clinically rated using the five-level UPDRS scores (i.e., 0, 1, 2, 3, 4). The detailed assessment conducted for each symptom was as follows (see Fig. 2):

1) *Elbow Rigidity*: with the subjects in a relaxed state and with their arm out, the examiner attempted to move the subject's forearm up and down in a cogwheel motion around their elbow trying to achieve a full range of motion. 2) *Wrist Rigidity*: with the subjects in a relaxed state and their arm out, the examiner attempted to move the subject's hand up and down in a cogwheel motion around their wrist trying to achieve a full range of motion. 3) *Bradykinesia*: the subjects were asked to first hold out the arm in front of them and then to pronate and supinate their hands as much as possible. Pronation-supination movements are considered to be equally important as finger tapping and hand grasp [13] and one of the most useful features [45] in assigning severity of bradykinesia. To a compact design of the sensor system set-up, pronation-supination movements are selected in this study. 4) *Kinetic Tremor*: the subjects were asked to use the index finger from the examined arm to touch their noses, and then to move that finger towards the examiner's own index finger which was approximately an arm's length distance. 5) *Postural Tremor*: the subjects held their arm out in front of them for 10 seconds. 6) *Rest Tremor*: the subjects stayed seated and relaxed placing their hands on their laps with their palms facing towards the ceiling.

C. Data Processing and Features Extraction

Leading up to the feature extraction, the measured signals such as accelerations and MMG signals were processed as follows: the measured accelerations were filtered using a 4th order Butterworth lowpass filter with cutoff frequencies at 25 Hz for all symptoms; the MMG signals were processed by the following steps: filtered using a 4th order Butterworth bandpass filter between 10 Hz and 100 Hz [43], rectified, filtered using a 4th order Butterworth lowpass filter with cutoff frequency of 5 Hz (see Fig.3). Note that the 4th order Butterworth filter was used in all following filtering processes. Table II describes all features used for rigidity, bradykinesia and tremor assessments, and Table III shows the features for each PD symptom assessment. The definitions and extractions of the features for assessing each symptom are detailed as follows:

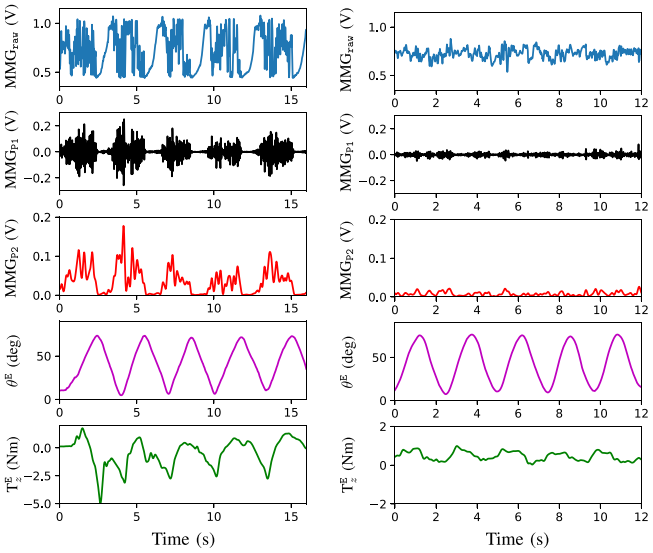

(a) PwPD (UPDS = 3) (b) Healthy subject

Fig. 3. Examples of the MMG signals measured from triceps brachii during elbow rigidity assessments (MMG_{raw}: raw MMG signal, MMG_{P1}: MMG signal processed after high-pass filter, MMG_{P2}: MMG signal processed after low-pass filter, θ^E: measured elbow joint angle, T_z^E: measured torque along the force sensor's z axis). (a) Results measured with a PwPD (UPDRS score = 3), (b) Results measured with a healthy subject.

TABLE II
FEATURES' DESCRIPTION

Features	*Description*
meanT:	Mean torques acting on wrist/elbow joint
stdT:	Standard deviations of the torques on wrist/elbow joint
meanA:	Mean processed linear IMU accelerations
stdA:	Standard deviations of processed linear IMU accelerations
meanV:	Mean angular velocities of wrist/elbow joints
stdV:	Standard deviation of wrist/elbow joint velocities
meanθ:	Mean wrist/elbow joint angles
stdθ:	Standard deviation of wrist/elbow joint angles
Freq:	Mean frequency of pronation/supination movements
meanMMG:	Mean processed MMG signals after low-pass filter
stdMMG:	Standard deviation of processed MMG signals

1) Rigidity Features: As the handle was used during the rigidity assessment, force-based features were extracted for quantifying the rigidity symptom (see Table II and III). With the force handle, the applied 2D torques (T_y and T_z, see Fig.1) on the subject's joint were first calculated. T_z plays the main role to move the subject's hand or forearm (see Fig. 3), and

TABLE III
FEATURES FOR EACH PD SYMPTOM

Symptom	*Features*
Wrist rigidity:	$\text{meanT}_y^{\text{W}}$, stdT_y^{W}, $\text{meanT}_z^{\text{W}}$, stdT_z^{W} $\text{mean}\theta^{\text{W}}$, $\text{std}\theta^{\text{W}}$, $\text{stdV}_{x,y,z}^{\text{W}}$ $\text{meanMMG}_{1,2}^{\text{F}}$, $\text{stdMMG}_{1,2}^{\text{F}}$
Elbow rigidity:	$\text{meanT}_y^{\text{E}}$, stdT_y^{E}, $\text{meanT}_z^{\text{E}}$, stdT_z^{E} $\text{mean}\theta^{\text{E}}$, $\text{std}\theta^{\text{E}}$, $\text{stdV}_{x,y,z}^{\text{E}}$ $\text{meanMMG}_{1,2}^{\text{U}}$, $\text{stdMMG}_{1,2}^{\text{U}}$
Bradykinesia:	$\text{stdV}_{x,y,z}^{\text{U,F}}$, $\text{stdV}_{x,y,z}^{\text{U,F}}$, Freq $\text{meanMMG}_{1,2}^{\text{U,F}}$, $\text{stdMMG}_{1,2}^{\text{U,F}}$,
$\text{Tremor}_{\text{K,P,R}}$:	$\text{stdA}_{x,y,z}^{\text{U,F}}$, $\text{stdV}_{x,y,z}^{\text{U,F}}$ $\text{meanMMG}_{1,2}^{\text{U,F}}$, $\text{stdMMG}_{1,2}^{\text{U,F}}$

The subscripts K, P, R represent the kinetic, postural and rest tremors, respectively.
The superscripts W, E, U, F represent the wrist, elbow, upper arm and forearm, respectively.
The subscripts x, y, z represent the x, y, z axes, respectively, 1, 2 the MMG number.

T_y was also used to give a general image of the relative torque around y axis between the handle and the subject's arm. The torque T_y and T_z around the wrist and elbow were estimated as

$$T_i = F_i L_i, \quad i \in \{y, z\} \tag{1}$$

where F_i shows the measured forces along y and z axes, and L_i denotes the related arm lengths of each force around the wrist and elbow.

In addition, resistance is a fundamental factor for clinicians when assessing rigidity, in particular, impedance and VEPs of the human joints have been revealed to be indicative of rigidity in PwPD [31], [35], [36], in which the joint impedance and VEPs were estimated using a regression method based on the measured torque, joint angular displacement (θ) and velocity ($\dot{\theta}$). In this study, these three elements were directly used as features to a machine learning algorithm instead of estimating the joint impedance and VEPs. The relative wrist and elbow joint angles were estimated as follows:

$$\theta = 2 \arccos((\boldsymbol{q}_m \boldsymbol{q}_n^{-1})_{[0]}) \tag{2}$$

where $\boldsymbol{q}$ denotes the quaternion of the IMU sensor, which was estimated using a gradient descent based fusion algorithm based on the measured 3D accelerations and 3D rate-of-turns [46]. m and n represent the two IMUs attached on the handle/forearm and the forearm/upper arm, respectively. The angular velocity $\dot{\theta}$ was directly extracted from the gyroscope sensor of the IMU since only one segment of the patient's arm such as hand or forearm was moved during the wrist or elbow rigidity assessment.

For each assessment of the rigidity, the force-based features consist of the mean and standard deviation of the calculated torque, the standard deviation of the joint angle and angular velocities. As rigidity is defined as involuntary, long-latency reflex muscle contractions, the mean and standard deviations of MMG readings from each rigidity assessment were used as features as well (see Table II and III). In Fig.3, it can be seen that significant MMG signals can be measured when the patients have high elbow rigidity (i.e., UPDRS = 3), while there exist no significant MMG signals with healthy subjects during elbow rigidity assessment.

2) Bradykinesia Features: Normally, the determining factors for bradykinesia severity include the speeds of pronation/supination movements, amplitudes of rotations, frequencies of hesitations and signs of decrementing amplitudes, etc [4]. During the pronation/supination movements, the measured rotation rates using the IMUs on the forearm and upper arm in three orthogonal axes were assumed to best represent bradykinesia severity. Similarly, the measured rotation rates were filtered using a Butterworth lowpass filter with cutoff frequency at 3 Hz to avoid the influence caused by a concomitant tremor. The standard deviation of the rotation rate was used to show the root mean square of pronation/supination motion speeds (the mean value is zero). The main frequency of the rotation rates of the arm was also calculated using the fast Fourier transformation (FFT) as a feature to indicate the motion frequency. Moreover, the mean and standard deviation of the MMG recordings were identified as integral features for bradykinesia because the related muscles controlled the hand/forearm pronation and supination motions (see Table II and III).

3) Tremor Features: Tremor severity is characterised by the amplitude of tremor. The higher the amplitude of tremor, the higher the UPDRS score associated with it. The IMU sensor comprises a gyroscope and an accelerometer (linear acceleration) both of which have been used to evaluate tremor [32], [47]. The raw data from the two IMUs' gyroscopes and accelerometers were filtered with a Butterworth bandpass filter (2 - 12 Hz) to remove artefacts caused by the patients' voluntary movements (e.g., kinetic tremor assessment motions) and the gravity in the measured accelerations. The means and standard deviations of processed rates-of-turn and accelerations were used as feature inputs for tremor classification. As EMG signals have also been shown as an effective means in assessing tremor previously [48], [49], the MMG data, i.e., the mean and standard deviation of the processed MMG signals, was also included as the features (see Table II and III).

D. Classification Method

A main objective of this study is to quantify the severity of PD symptoms, which is represented by the UPDRS scores rated by the clinicians, based on the extracted features as shown in Table III (i.e., *UPDRS classification*). To this end, a voting classification model was developed by combining three base classifiers: a 1-nearest neighbour (1-NN) classifier, a multi-layer perceptron (MLP) neural networks classifier, and an AdaBoost classifier. The three base classifiers were selected based on a pre-selection process in which 13 common classification methods [50] were tested including K nearest neighbours (KNN, K = 1,3,5), Linear SVM, Quadratic SVM, Cubic SVM, RBF SVM, Simple Tree, Medium Tree, Complex Tree, Random Tree, MPL neural networks and AdaBoost Classifier. The pre-selection process followed the same model training and validation steps of the proposed voting classification model (see Section II-D.1) by taking into account the evaluation accuracy and variance of each classifier. The results

TABLE IV
ACCURACIES OF THE VOTING CLASSIFIER AND THE TOP-FIVE-RANKED CLASSICAL CLASSIFIERS

Models	Accuracy For Each Symptom - *With All Features* ([mean (95% confidence interval)], unit:%)						
	Elbow Rigidity	Wrist Rigidity	Bradykinesia	Kinetic Tremor	Postural Tremor	Rest Tremor	Average
KNN (K=1)	92.7 (11.1)	86.4 (13.9)	85.8 (7.3)	89.9 (10.6)	79.6 (20.2)	76.3 (11.0)	85.1
AdaBoost	81.7 (10.0)	81.1 (6.8)	78.9 (6.1)	88.2 (7.1)	79.9 (19.4)	84.3 (12.8)	83.0
Neural Network	89.5 (14.1)	82.2 (18.0)	80.7 (6.8)	90.0 (8.4)	74.1 (9.2)	76.4 (16.8)	81.9
KNN (K=3)	72.9 (17.1)	67.1 (21.5)	74.2 (19.5)	87.3 (10.4)	68.4 (30)	71.8 (7.9)	73.6
Random Forest	69 (24.0)	65.7 (8.1)	73.8 (15.0)	73.8 (10.3)	77.5 (21.6)	74.6 (15.2)	72.4
Voting Classifier	89.6 (15.7)	88.4 (10.7)	85.1 (6.8)	91.8 (10.6)	80.2 (13.7)	80.1 (16.1)	85.4

are detailed in the Section III. The three classifiers with top three accuracies (averaged across all symptoms) were selected and integrated using the voting classification algorithm [50]. Since the 1-NN classifier regularly ranked the highest amongst the 13 classical classifiers, so it was selected as the base classifier. Due to its high variance nature, when faced with a much larger training set, 1-NN's over-fitting nature and the model complexity may prove detrimental. However, the voting classifier has a lower risk of over-fitting because of its numerous base classifiers. Using the voting classifier, each of the base classifiers generated a predictive probability output and a final UPDRS score was selected using the soft voting algorithm in which the largest sum of predictive probabilities from each classifier for each UPDRS class was used. Hence, the proposed voting classification method can ensure better robustness and higher accuracy across the assessments of all symptoms compared to using each single classifier even though they have shown relatively high accuracy for certain symptom assessments (see Table IV).

It should be noted that the UPDRS scores rated by the clinicians are still subject to inter- and intra-rater subjectivity. To further reduce the subjectivity and evaluate the effectiveness of the proposed voting classification method, an experiment was conducted to distinguish the PwPD (i.e., UPDRS $>$ 0) from healthy subjects (control group) (i.e., *PwPD-HS classification*). Note that the UPDRS scores of PwPD can be rated as zero when appropriated DBS settings are given.

1) Model Training and Validation: During the training phase of the *UPDRS classification*, each classification model was trained using the total dataset for each symptom to optimise the hyper-parameters, e.g., its complexity or speed of learning, to ensure high performance (see Section II-D.2) of each classification model. Each patient was asked to perform the motions three times for each symptom assessment and 8 patients participated in the experiments multiple times during their DBS treatments. The total number of UPDRS labels for each symptom are as follows: elbow rigidity: 98; wrist rigidity: 96; bradykinesia: 114; kinetic tremor: 110; postural tremor: 115; rest tremor: 156. Note that the cases with UPDRS $= 4$ have been removed for each symptom assessment due to the insufficient number ($<$4) for classification. The hyper-parameters of the three base classifiers were selected as follows: for the KNN (K $= 1$), the brute-force search was selected to compute the nearest neighbours; for the AdaBoost classifier, the decision tree (maximum depth $= 4$) was used as the base classifier, the number of estimators and the learning rate were set as 1000 and 1.5, respectively; for the MPL neural network classifier, one hider layer with size $= 100$ was used, and the maximum number of iterations and the α parameters were set as 2000 and 0.1, respectively. The weights of three base classifiers, 1-NN, AdaBoost, and MLP neural networks, were set as 1, 4 and 2, respectively. The performance of the voting classifier depends mainly on the AdaBoost and then the MLP neural networks, finally the 1-NN. In the evaluation phase, the final score of each classifier was calculated by averaging over each of the results of a 5-fold cross-validation procedure [50].

In terms of the *PwPD-HS classification*, the total number of labels for each group are as follows (HS:PwPD (UPDRS$>$0)): 30:71 (elbow rigidity), 30:62 (wrist rigidity), 30:91 (bradykinesia), 30:60 (kinetic tremor), 30:76 (postural tremor), and 30:92 (rest tremor). The hyper-parameters of the classification model were set as the same used for the UPDRS classification. In addition, the 5-fold cross-validation procedure was also selected for evaluation.

2) Model Performance: To evaluate the performance, the accuracy score was used and calculated as follows:

$$\texttt{Accuracy} = \frac{N_T}{N_{all}} \times 100\% \tag{3}$$

where N_T denotes the number of correctly detected labels (i.e., UPDRS scores for *UPDRS classification* or PD states for *PwPD-HS classification*), N_{all} shows the total number of the labels used for evaluation.

III. RESULTS

A. Accuracy of UPDRS Classification

As mentioned in Section II-D, the voting classification method was designed based on three base classifiers which were selected from 13 applicable classifiers. During such process, the accuracy of each classifier for was obtained utilising all features for each symptom, i.e., with no feature dimensionality reduction. Table IV shows the top-five-ranked classifiers among all classifiers for each PD symptom based on the average accuracy scores across all symptoms. For each symptom, the accuracy score of each classifier was calculated using the 5-fold cross-validation procedure. Among the 13 classical machine learning algorithms, the top-five-ranked ones are as follows: 1-NN, AdaBoost, Neural network, 3-NN, and RBF SVM. The voting classification algorithm was designed based on the three-highest ranked ones and show the best average accuracy (85.4%) across all symptoms. Moreover, the best performance in estimating the UPDRS scores for each

TABLE V
THE FIVE MOST RELEVANT FEATURES FOR EACH SYMPTOM

Symptoms	Features									
	1st	2nd	3rd	4th	5th	Correlation Coefficients (CC)				
Elbow Rigidity*	$\text{std}T_y^{\text{E}}$	$\text{mean}T_y^{\text{E}}$	$\text{std}V_z^{\text{E}}$	$\text{mean}\theta^{\text{E}}$	$\text{std}\theta^{\text{E}}$	[6.9	6.6	6.6	5.6	5.5]
Wrist Rigidity	$\text{std}V_y^{\text{W}}$	$\text{meanMMG}_1^{\text{F}}$	$\text{stdMMG}_1^{\text{F}}$	$\text{std}\theta^{\text{W}}$	$\text{mean}T_y^{\text{W}}$	[19.3	7.4	5.7	5.4	5.2]
Bradykinesia	$\text{std}V_y^{\text{F}}$	$\text{std}V_x^{\text{F}}$	Freq_y^{F}	$\text{meanMMG}_2^{\text{U}}$	$\text{stdMMG}_2^{\text{U}}$	[30.4	16.9	14.1	11.0	10.1]
Kinetic Tremor	stdV_z^{U}	stdV_x^{U}	stdA_y^{F}	$\text{meanMMG}_1^{\text{U}}$	stdV_x^{F}	[6.9	5.7	5.7	5.5	5.4]
Postural Tremor	$\text{stdMMG}_1^{\text{F}}$	$\text{meanMMG}_1^{\text{F}}$	stdA_z^{U}	$\text{meanMMG}_1^{\text{U}}$	stdV_y^{U}	[62.6	57.6	38.9	37.3	36.8]
Rest Tremor	$\text{meanMMG}_2^{\text{U}}$	stdA_y^{F}	stdA_x^{F}	stdA_x^{U}	stdA_z^{U}	[73.2	63.9	56.1	50.7	49.6]

*$\text{stdMMG}_2^{\text{U}}$ is the 6th most relevant feature (CC=4.2).

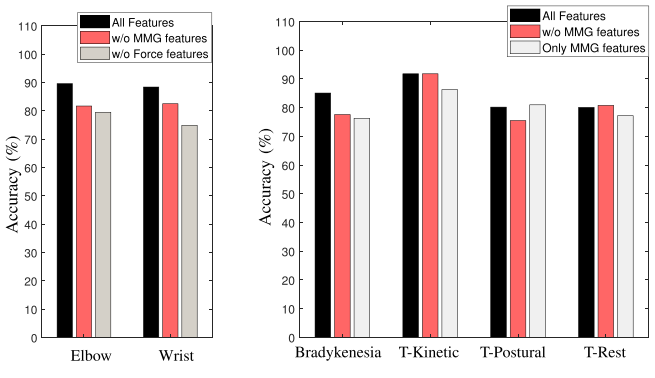

(a) Rigidity (b) Bradykenesia and Tremor (T)

Fig. 4. Classification accuracies using the voting classifier under three conditions: all features, without MMG-based features and without force-based features (rigidity)/only MMG-based features (bradykenesia and tremor).

symptom were all obtained by the voting classifier or one of its three base classifiers. The voting classifier shows the highest accuracy for estimating the UPDRS scores for wrist rigidity (accuracy = 88.4%), kinetic tremor (accuracy = 91.8%), and postural tremor (accuracy = 80.2%), and the second-highest accuracy for remaining symptoms such as elbow rigidity (89.6% vs 92.7%, voting classifier vs 1-NN), bradykinesia (85.1% vs 85.8%, voting classifier vs 1-NN), and rest tremor (80.1% vs 84.3%, voting classifier vs AdaBoost).

B. Contributions of the MMG Signals

To investigate the use of the MMG signals in improving the accuracy, the correlation coefficient between each feature and the UPDRS scores was calculated using the ANOVA analysis. The five most relevant features for each symptom and their correlation coefficients are shown in Table V. It can be observed that the MMG based features contribute at least one of the five most relevant features for all symptoms except for the elbow rigidity, for which the $\text{stdMMG}_2^{\text{U}}$ is the sixth most relevant features. The MMG based features show high correlations to the UPERS scores for postural and rest tremors.

A further comparison study was conducted to evaluate whether the rigidity UPDRS scores can be estimated using only MMG and IMU-based features so that the force handle can be removed in the clinical assessment. Fig.4(a) shows the classification accuracies for wrist/elbow rigidities using the voting classifier under three conditions: all features, without MMG-based features, without force-based features. It can be observed that the classification accuracy is significantly reduced by removing force-based or MMG-based features compared to that using all features. The removal of the force-based and MMG-based features respectively reduces the accuracy by 10.1% and 7.9 % for elbow rigidity and by 13.5% and 5.9% for wrist rigidity. In other words, by comparing the reduction of accuracies caused by separately removing the force-based and MMG-based features, it can be noted that MMG-based features show the similar effort as the force-based ones (79.5% vs 81.7%) for the elbow rigidity assessments, but less effect for wrist rigidity assessment (74.9% vs 82.5%).

A similar study was carried out to compare the performances of the voting classifier separately using all sensor features excluding MMG-based features and only MMG-based features for bradykinesia and tremor assessments. Fig. 4(b) shows the classification accuracies under three conditions: all features, without MMG-based features and only MMG-based features. Compared to using all features, the removal of MMG-based features does not affect the classification accuracy for kinetic tremor (all features vs without MMG: 91.8% vs 91.8%) and rest tremor (all features vs without MMG: 80.1% vs 80.8%) assessments, but lowers the classification accuracy for bradykinesia (all features vs without MMG: 85.1% vs 77.6%) and postural tremor (all features vs without MMG: 80.2% vs 75.5%) assessments. Although the MMG-based features show high correlations with the UPDRS scores for rest tremor assessments (see Table V), the removal of MMG-based features does not significantly affect the classification accuracy (see Table 4(b)). This is because the remaining features have also high correlation coefficients with the UPDRS scores. In addition, it can be seen that using only the MMG-based features shows the similar accuracy for bradykinesia and tremor assessments as the IMU-based features (bradykinesia: 76.3% vs 77.6%, kinetic tremor: 86.3% vs 91.8%, postural tremor: 81.0% vs 75.5%; rest tremor: 77.2% vs 80.8%).

C. Confusion Matrix of UPDRS Classification

Fig. 5 shows the confusion matrices of the estimated UPDRS scores of six symptoms when using the voting classifier. The classification confusion mainly occurs between the neighbouring UPDRS scores for bradykinesia and kinetic tremor assessments. For the assessments of elbow rigidity, wrist rigidity and postural tremor, these exist limited classification confusions ($\leq$3) between two UPDRS scores with

TABLE VI
ACCURACIES OF THE HS-PWPD (UPDRS>0) AND PWPD (UPDRS=0)-PWPD (UPDRS>0) CLASSIFICATIONS

Datasets	Accuracy For Each Symptom - *With All Features* ([mean (95% confidence interval)], unit:%)						
	Elbow Rigidity	Wrist Rigidity	Bradykinesia	Kinetic Tremor	Postural Tremor	Rest Tremor	Average
$HS/PwPD_{[1,2,3]}$	95.0 (11.0)	98.9 (4.4)	96.7 (9.7)	97.8 (8.9)	95.3 (6.0)	96.0 (7.2)	96.6
$PwPD_{[0]}/PwPD_{[1,2,3]}$	90.8 (10.2)	90.7(15.3)	91.1 (11.0)	89.9 (10.6)	85.2 (15.2)	86.5 (8.7)	89.0

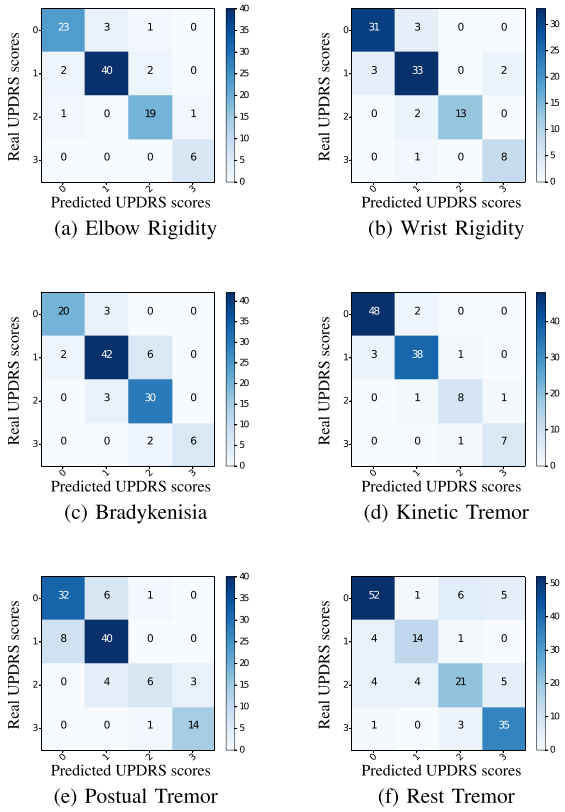

(a) Elbow Rigidity (b) Wrist Rigidity (c) Bradykenisia (d) Kinetic Tremor (e) Postual Tremor (f) Rest Tremor

Fig. 5. Confusion matrices for all symptoms with using the voting classifier.

the difference is 2, and no classification confusion between two UPDR scores with higher differences. In the classification results for rest tremor, relatively significant confusion occurs between two UPDRS scores with the difference is 2 (10 times) and higher (6 times).

D. Accuracy of PwPD-HS Classification

In the aforementioned experiments, the 5-level UPDRS scores rated by clinicians were used as the gold standard for classification. In this experiment, all features with PwPD (UPDRS $>$ 0, i.e., $PwPD_{[1,2,3]}$) were defined as one group and a new healthy subject cohort was included as the control group. The proposed features and voting classification method were further evaluated to distinguish the PD patients from healthy subjects. Table VI shows that high classification accuracies (96.6% on average across all symptoms) can be achieved for all symptom assessment. Moreover, the symptoms of the PwPD can be removed or largely reduced to an insignificant level with appropriate DBS, and correspondingly, the UPDRS scores were rated as 0 by clinicians. Besides, some PwPD show only one or two symptoms. The data collected with PwPD under these two cases (i.e., UPDRS $= 0$) were also classified as one group ($PwPD_{[0]}$). Similarly, the voting classification method was used to distinguish such group (i.e., $PwPD_{[0]}$) patients from the $PwPD_{[1,2,3]}$ group. Average classification accuracy of 89% across all symptoms can also be obtained, however, 7.6% less than that between the control group and the $PwPD_{[1,2,3]}$ group.

IV. DISCUSSION

We have designed, fabricated, programmed, and clinically tested a wearable sensor system, a Parkinson's diagnostic device, capable of measuring all three cardinal motor symptoms of Parkinson's Disease. We have further introduced a new sensing modality, MMG, as well as a new wearable MMG sensor that extracts important features of all PD symptoms. Based on the extracted features, a voting classification algorithm was developed to quantify the PD symptoms according to the UPDRS scores rated by clinicians. The developed system was able to classify the UPDRS scores of three cardinal PD motor symptoms with an average accuracy of 85.4%. Moreover, an average classification accuracy of 96.6% can be achieved when using the developed system to distinguish the PD patients from healthy subjects. The results also reveal that the use of the MMG-based features effectively improves the general accuracy by $7.1 \pm 1.1\%$ for rigidity and bradykinesia assessments. Of particular note, we found that the designed wearable armband consists of an IMU sensor and two MMG sensors has the potential to quantify rigidity symptom by replacing the force sensor, although a difference was observed in the results when used for assessing elbow rigidity (accuracy $=$ 79.5%) and wrist rigidity (accuracy $=$ 74.9%). Furthermore, the MMG-based features show a similar effect (i.e., accuracy) for UPDRS classification as the IMU-based features for tremor assessments ($81.5 \pm 4.6\%$ vs $82.7 \pm 8.3\%$).

UPDRS is the current gold-standard in measuring symptom severity in PD in this study. Hence, the classification results are comparable to clinician rating, in particular, for elbow/wrist rigidity and kinetic tremor which yield an average accuracy of $89.9 \pm 1.7\%$. The prediction accuracies of UPDRS scores for postural and rest tremors (80.2% and 80.1%, respectively) are comparable to current studies (e.g., kinetic tremor: 77.4%, postural tremor: 79.3%, rest tremor: 78.6%, [5-fold cross-evaluation accuracy] [51]). In [51], a regression method was used based on the arm linear accelerations and rates of turn measured using IMU sensors. Finally, the developed system is able to distinguish the PD patients from healthy subjects with high accuracy (96.6%) across all symptom assessments. In general, the results imply that the sensor system meets or exceeds current standards in PD symptoms assessment. The results also show promise to adapt to improved

(e.g., higher resolution, multi-dimensional) rating scales proposed for more precise disease assessment. Past studies have targeted only one or two main PD symptoms [39], [40]. This is the first investigation introducing a sensor system with the capacity to measure all three cardinal symptoms on a significantly sized PD cohort. Moreover, although existing studies have shown EMG can be used for the assessment of Parkinsonian rigidity [52], this study performed the first trial to use MMG signals to classify the 5-level UPDRS scores.

We propose an expanded study in terms of patient and clinician numbers in future work for subsequent system translation. In the current patient cohort, numbers of cases with UPDRS score = 2 and/or 3 were low for all PD symptoms except for the rest tremor (see Fig.5), and no patients had the rare condition of a UPDRS score = 4 for all symptoms. The system also holds a strong future potential to address inter- and intra-rater subjectivity across PD examiners, however the number of testing physicians needs to be expanded to explore this capability. To reduce the subjectivity in this investigation, a control group was included. Results comparing the control subjects to PwPD demonstrates very high classification accuracy (96.6%, on average across all symptoms). It is noteworthy that some PwPD's PD symptoms were rated as zero (most of them under DBS) and $\text{PwPD}_{[0]}$ group can still be accurately distinguished from the $\text{PwPD}_{[1,2,3]}$ group very reliably (89%), which approaches the very high accuracy (96.6%) distinction between control and PD patients.

The new sensing modality also opens many rich areas for future study. For instance, a normalization of the MMG signals across patients can improve the diagnosis by asking the patient to perform several prescribed motions before clinical assessment. A larger dataset can be built to reduce the errors in the UPDRS scores rated by clinicians and improve the accuracy of the model. Note that this study also focused on the most-affected side of the patients' arms. Bilateral experiments and feature ranking strategies [45], [53], in particular out-of-clinic, could lend critical insights to disease progression and treatment efficacy. Results demonstrating MMG can measure rigidity enable significant system size reduction which can further enable long ambulatory assessments for home use and extraction of information related to activities of daily living. Moreover, with a smaller version, the system can also be easily placed on other body segments, for example, placing an IMU on the hand can extract more features for bradykinesia and tremor assessment since these symptoms are more distal. Furthermore, the IMU-MMG based system can also be further developed for lower limbs to monitor some important features of PD, e.g., gait and postural instability, which cannot be measured using the current system.

V. Conclusion

This investigation has introduced the first wearable system capable of measuring all three cardinal motor symptoms of Parkinson's disease as correlated with clinician standard UPDRS scores. The developed sensor system consists of a force-sensor handle, three IMUs and four novel MMG sensors. The system is compact and can be easily used during clinical or home-based assessments. System use does not require any expertise and can be done without any clinical training. The results have shown that high classification accuracies across all symptoms can be achieved using the developed system. We have further shown that the use of MMG-based features can effectively improve the accuracies for assessing the rigidity, bradykinesia, and kinetic tremor. Moreover, the comparison study has revealed that MMG-based features show the potential to quantify rigidity comparably to force measurement. In future work, the sensor system will be adjusted to be used at home to monitor symptoms away from the hospitalenabling regular "on-the-fly" treatment adjustments and full telemedicine. This holds very significant potential to extend the efficacy of pharmaceutical and DBS treatments whose dosage and stimulation level are prescribed only based on limited "snapshots" of clinician time. Furthermore, this can provide a closed-loop feedback system to allow for individualised treatment for motor fluctuations in PwPD, particularly those who have had DBS where the stimulation output can be adjusted according to symptoms variation. This investigation has triggered clinical work aimed at translation. The sensing system has been successfully patented [54] and a new venture, Serg Technologies, has been formed to commercialize the system for widespread patient use.

Acknowledgment

The authors would like to thank all subjects for their willingness to participate in the study and the clinicians at Charing Cross Hospital, London, U.K., and John Radcliffe Hospital, Oxford, U.K., for their help in PD assessments.

References

[1] R. L. Nussbaum and C. E. Ellis, "Alzheimer's disease and Parkinson's disease," *New England J. Med.*, vol. 348, no. 14, pp. 1356–1364, 2003.
[2] *Statistics on Parkinson's—Parkinson's Disease Foundation*. Accessed: Jan. 23, 2020. [Online]. Available: https://www.parkinson.org/Understanding-Parkinsons/Statistics
[3] W. Dauer and S. Przedborski, "Parkinson's disease: Mechanisms and models," *Neuron*, vol. 39, no. 6, pp. 889–909, 2003.
[4] J. Jankovic, "Parkinson's disease: Clinical features and diagnosis," *J. Neurol., Neurosurg. Psychiatry*, vol. 79, no. 4, pp. 368–376, 2008.
[5] M. B. Shapiro, D. E. Vaillancourt, M. M. Sturman, L. V. Metman, R. A. E. Bakay, and D. M. Corcos, "Effects of STN DBS on rigidity in Parkinson's disease," *IEEE Trans. Neural Syst. Rehabil. Eng.*, vol. 15, no. 2, pp. 173–181, Jun. 2007.
[6] A. Rabie *et al.*, "Improvement of advanced Parkinson's disease manifestations with deep brain stimulation of the subthalamic nucleus: A single institution experience," *Brain Sci.*, vol. 6, no. 4, p. 58, 2016.
[7] A. Salarian, H. Russmann, C. Wider, P. R. Burkhard, F. J. G. Vingerhoets, and K. Aminian, "Quantification of tremor and bradykinesia in Parkinson's disease using a novel ambulatory monitoring system," *IEEE Trans. Biomed. Eng.*, vol. 54, no. 2, pp. 313–322, Feb. 2007.
[8] K. Kostoglou, K. P. Michmizos, P. Stathis, D. Sakas, K. S. Nikita, and G. D. Mitsis, "Classification and prediction of clinical improvement in deep brain stimulation from intraoperative microelectrode recordings," *IEEE Trans. Biomed. Eng.*, vol. 64, no. 5, pp. 1123–1130, May 2017.
[9] I. M. Germano, J.-M. Gracies, D. J. Weisz, W. Tse, W. C. Koller, and C. W. Olanow, "Unilateral stimulation of the subthalamic nucleus in Parkinson disease: A double-blind 12-month evaluation study," *J. Neurosurg.*, vol. 101, no. 1, pp. 36–42, Jul. 2004.
[10] M. Picillo *et al.*, "Dystonia as complication of thalamic neurosurgery," *Parkinsonism Rel. Disorders*, vol. 66, pp. 232–236, Sep. 2019.
[11] T. Mera, J. L. Vitek, J. L. Alberts, and J. P. Giuffrida, "Kinematic optimization of deep brain stimulation across multiple motor symptoms in Parkinson's disease," *J. Neurosci. Methods*, vol. 198, no. 2, pp. 280–286, Jun. 2011.

[12] T. Tykocki, P. Nauman, H. Koziara, and T. Mandat, "Microlesion effect as a predictor of the effectiveness of subthalamic deep brain stimulation for Parkinson's disease," *Stereotactic Funct. Neurosurg.*, vol. 91, no. 1, pp. 12–17, 2013.

[13] C. G. Goetz *et al.*, "Movement disorder society-sponsored revision of the unified Parkinson's disease rating scale (MDS-UPDRS): Scale presentation and clinimetric testing results," *Movement Disorders*, vol. 23, no. 15, pp. 2129–2170, Nov. 2008.

[14] B. Post, M. P. Merkus, R. M. A. de Bie, R. J. de Haan, and J. D. Speelman, "Unified Parkinson's disease rating scale motor examination: Are ratings of nurses, residents in neurology, and movement disorders specialists interchangeable?" *Movement Disorders*, vol. 20, no. 12, pp. 1577–1584, Dec. 2005.

[15] B.-R. Chen *et al.*, "A Web-based system for home monitoring of patients with Parkinson's disease using wearable sensors," *IEEE Trans. Biomed. Eng.*, vol. 58, no. 3, pp. 831–836, Mar. 2011.

[16] W. Maetzler, J. Domingos, K. Srulijes, J. J. Ferreira, and B. R. Bloem, "Quantitative wearable sensors for objective assessment of Parkinson's disease," *Movement Disorders*, vol. 28, no. 12, pp. 1628–1637, Oct. 2013.

[17] S. Patel *et al.*, "Monitoring motor fluctuations in patients with Parkinson's disease using wearable sensors," *IEEE Trans. Inf. Technol. Biomed.*, vol. 13, no. 6, pp. 864–873, Nov. 2009.

[18] L. di Biase *et al.*, "Quantitative analysis of bradykinesia and rigidity in Parkinson's disease," *Frontiers Neurol.*, vol. 9, p. 121, Mar. 2018.

[19] R. I. Griffiths *et al.*, "Automated assessment of bradykinesia and dyskinesia in Parkinson's disease," *J. Parkinson's Disease*, vol. 2, no. 1, pp. 47–55, 2012.

[20] R. A. Ramdhani, A. Khojandi, O. Shylo, and B. H. Kopell, "Optimizing clinical assessments in Parkinson's disease through the use of wearable sensors and data driven modeling," *Frontiers Comput. Neurosci.*, vol. 12, Sep. 2018.

[21] F. Widjaja, C. Y. Shee, W. L. Au, P. Poignet, and W. T. Ang, "Towards a sensing system for quantification of pathological tremor," in *Proc. Int. Conf. Intell. Adv. Syst.*, Nov. 2007, pp. 3250–3255.

[22] R. LeMoyne, T. Mastroianni, M. Cozza, C. Coroian, and W. Grundfest, "Implementation of an iPhone for characterizing Parkinson's disease tremor through a wireless accelerometer application," in *Proc. Annu. Int. Conf. IEEE Eng. Med. Biol.*, Aug. 2010, pp. 4954–4958.

[23] H. Dai, P. Zhang, and T. Lueth, "Quantitative assessment of parkinsonian tremor based on an inertial measurement unit," *Sensors*, vol. 15, no. 10, pp. 25055–25071, 2015.

[24] S. F. Atashzar, M. Shahbazi, O. Samotus, M. Tavakoli, M. S. Jog, and R. V. Patel, "Characterization of upper-limb pathological tremors: Application to design of an augmented haptic rehabilitation system," *IEEE J. Sel. Topics Signal Process.*, vol. 10, no. 5, pp. 888–903, Aug. 2016.

[25] J. P. Giuffrida, D. E. Riley, B. N. Maddux, and D. A. Heldman, "Clinically deployable Kinesia technology for automated tremor assessment," *Movement Disorders, Off. J. Movement Disorder Soc.*, vol. 24, no. 5, pp. 723–730, 2009.

[26] K. Sailunaz, E. Rupu, R. Vaidyanathan, S. Wang, and K. A. Mamun, "PVDoctor: Cloud based virtual doctor for Parkinson's disease screening and monitoring," in *Proc. IEEE Int. Conf. Eng. Med. Biol. (EMBC)*, Aug. 2016, pp. 1733–1736.

[27] M. H. Li, T. A. Mestre, S. H. Fox, and B. Taati, "Vision-based assessment of parkinsonism and levodopa-induced dyskinesia with pose estimation," *J. NeuroEng. Rehabil.*, vol. 15, no. 1, p. 97, Dec. 2018.

[28] C.-W. Cho, W.-H. Chao, S.-H. Lin, and Y.-Y. Chen, "A vision-based analysis system for gait recognition in patients with Parkinson's disease," *Expert Syst. Appl.*, vol. 36, no. 3, pp. 7033–7039, Apr. 2009.

[29] A. P. Rocha, H. Choupina, J. M. Fernandes, M. J. Rosas, R. Vaz, and J. P. S. Cunha, "Kinect v2 based system for Parkinson's disease assessment," in *Proc. 37th Annu. Int. Conf. IEEE Eng. Med. Biol. Soc. (EMBC)*, Aug. 2015, pp. 1279–1282.

[30] N. Baradaran *et al.*, "Parkinson's disease rigidity: Relation to brain connectivity and motor performance," *Frontiers Neurol.*, vol. 4, p. 67, Jun. 2013.

[31] B. Kyu Park *et al.*, "Analysis of viscoelastic properties of wrist joint for quantification of parkinsonian rigidity," *IEEE Trans. Neural Syst. Rehabil. Eng.*, vol. 19, no. 2, pp. 167–176, Apr. 2011.

[32] H. Dai, B. Otten, J. H. Mehrkens, L. T. D'Angelo, and T. C. Lueth, "A novel glove monitoring system used to quantify neurological symptoms during deep-brain stimulation surgery," *IEEE Sensors J.*, vol. 13, no. 9, pp. 3193–3202, Sep. 2013.

[33] J. Levin, S. Krafczyk, P. Valkovič, T. Eggert, J. Claassen, and K. Bötzel, "Objective measurement of muscle rigidity in parkinsonian patients treated with subthalamic stimulation," *Movement Disorders*, vol. 24, no. 1, pp. 57–63, Jan. 2009.

[34] C. Ossig *et al.*, "Wearable sensor-based objective assessment of motor symptoms in Parkinson's disease," *J. Neural Transmiss.*, vol. 123, no. 1, pp. 57–64, Jan. 2016.

[35] A. Prochazka *et al.*, "Measurement of rigidity in Parkinson's disease," *Movement Disorders, Off. J. Movement Disorder Soc.*, vol. 12, no. 1, pp. 24–32, 1997.

[36] S. K. Patrick, A. A. Denington, M. J. A. Gauthier, D. M. Gillard, and A. Prochazka, "Quantification of the UPDRS rigidity scale," *IEEE Trans. Neural Syst. Rehabil. Eng.*, vol. 9, no. 1, pp. 31–41, Mar. 2001.

[37] J.-W. Kim *et al.*, "Regression models for the quantification of parkinsonian bradykinesia," *Bio-Med. Mater. Eng.*, vol. 26, no. s1, pp. S2249–S2258, Aug. 2015.

[38] G. Cai *et al.*, "Quantitative assessment of parkinsonian tremor based on a linear acceleration extraction algorithm," *Biomed. Signal Process. Control*, vol. 42, pp. 53–62, Apr. 2018.

[39] M. Memedi, J. Westin, D. Nyholm, M. Dougherty, and T. Groth, "A Web application for follow-up of results from a mobile device test battery for Parkinson's disease patients," *Comput. Methods Programs Biomed.*, vol. 104, no. 2, pp. 219–226, Nov. 2011.

[40] Z. Lin, H. Dai, Y. Xiong, X. Xia, and S.-J. Horng, "Quantification assessment of bradykinesia in Parkinson's disease based on a wearable device," in *Proc. 39th Annu. Int. Conf. IEEE Eng. Med. Biol. Soc. (EMBC)*, Jul. 2017, pp. 803–806.

[41] B. M. Eskofier *et al.*, "Recent machine learning advancements in sensor-based mobility analysis: Deep learning for Parkinson's disease assessment," in *Proc. 38th Annu. Int. Conf. IEEE Eng. Med. Biol. Soc. (EMBC)*, Aug. 2016, pp. 655–658.

[42] C. Kotsavasiloglou, N. Kostikis, D. Hristu-Varsakelis, and M. Arnaoutoglou, "Machine learning-based classification of simple drawing movements in Parkinson's disease," *Biomed. Signal Process. Control*, vol. 31, pp. 174–180, Jan. 2017.

[43] R. B. Woodward, S. J. Shefelbine, and R. Vaidyanathan, "Pervasive monitoring of motion and muscle activation: Inertial and mechanomyography fusion," *IEEE/ASME Trans. Mechatronics*, vol. 22, no. 5, pp. 2022–2033, Oct. 2017.

[44] S. Wilson *et al.*, "Formulation of a new gradient descent MARG orientation algorithm: Case study on robot teleoperation," *Mech. Syst. Signal Process.*, vol. 130, pp. 183–200, Sep. 2019.

[45] H. Reichmann, "Clinical criteria for the diagnosis of Parkinson's disease," *Neuro-Degenerative Diseases*, vol. 7, no. 5, p. 284, 2010.

[46] S. O. H. Madgwick, A. J. L. Harrison, and R. Vaidyanathan, "Estimation of IMU and MARG orientation using a gradient descent algorithm," in *Proc. IEEE Int. Conf. Rehabil. Robot.*, Jun. 2011, pp. 1–7.

[47] G. Rigas *et al.*, "Tremor UPDRS estimation in home environment," in *Proc. 38th Annu. Int. Conf. IEEE Eng. Med. Biol. Soc. (EMBC)*, Aug. 2016, pp. 3642–3645.

[48] F. Widjaja, C. Y. Shee, W. L. Au, P. Poignet, and W. T. Ang, "An extended Kalman filtering of accelerometer and surface electromyography data for attenuation of pathological tremor," in *Proc. 2nd IEEE RAS EMBS Int. Conf. Biomed. Robot. Biomechtron.*, Oct. 2008, pp. 193–198.

[49] V. Ruonala, A. Meigal, S. M. Rissanen, O. Airaksinen, M. Kankaanpää, and P. A. Karjalainen, "EMG signal morphology and kinematic parameters in essential tremor and Parkinson's disease patients," *J. Electromyogr. Kinesiol.*, vol. 24, no. 2, pp. 300–306, Apr. 2014.

[50] F. Pedregosa *et al.*, "Scikit-learn: Machine learning in Python," *J. Mach. Learn. Res.*, vol. 12, pp. 2825–2830, Oct. 2011.

[51] A. Haddock, K. T. Mitchell, A. Miller, J. L. Ostrem, H. J. Chizeck, and S. Miocinovic, "Automated deep brain stimulation programming for tremor," *IEEE Trans. Neural Syst. Rehabil. Eng.*, vol. 26, no. 8, pp. 1618–1625, Aug. 2018.

[52] J. Marusiak, A. Jaskólska, M. Koszewicz, S. Budrewicz, and A. Jaskólski, "Myometry revealed medication-induced decrease in resting skeletal muscle stiffness in Parkinson's disease patients," *Clin. Biomechanics*, vol. 27, no. 6, pp. 632–635, Jul. 2012.

[53] L. Gupta, S. Kota, S. Murali, D. L. Molfese, and R. Vaidyanathan, "A feature ranking strategy to facilitate multivariate signal classification," *IEEE Trans. Syst., Man, Cybern. C, Appl. Rev.*, vol. 40, no. 1, pp. 98–108, Jan. 2010.

[54] R. Vaidyanathan, N. Nowlan, R. Woodward, and S. Shefelbine, "Biomechanical activity monitoring," U.S. Patent 10 335 080, Jul. 2, 2019.